Fast Classification of Non-magnetic Metal Targets using Eddy-Current Based Impedance Spectroscopy

DOI:
10.1109/ICSENS.2017.8234219

Document Version
Accepted author manuscript

Published in:
2017 IEEE SENSORS

Fast Classification of Non-magnetic Metal Targets using Eddy-Current Based Impedance Spectroscopy

Michael D. O'Toole, Noushin Karimian and Anthony J. Peyton
School of Electrical and Electronic Engineering
The University of Manchester
Manchester, M13 9PL, UK
Email: michael.otoole@manchester.ac.uk

***Abstract*—We present a new method to sort non-magnetic conductive metals - specifically brass, copper and aluminium - with the aim of improving economic yields in the scrap metal and recycling industries. The method uses the impedance spectra of the metal objects derived from the scattered magnetic field. Preliminary results are presented on a small sample set showing good accuracy across all metal classes even when the test objects are travelling at high speeds (1 m/s). The results suggest the method is both feasible and practical at the high-throughput demanded by industry.**

***Keywords*—Waste recovery, Electromagnetic induction.**

I. Introduction

The safe and efficient reuse, recycling and recovery of waste metal from scrap is a significant issue with increasing economic and environmental implications. More than 50 million vehicles reach their end of life around the world every year producing huge quantities of scrap and material. Within the EU, current regulations mandate a ambitious target to recover 95% of material. Currently, the figure is around 75% [1].

A number of methods exist to identify and sort ferrous metals - mainly using large and powerful static magnetic fields. Non-magnetic metals however, pose a particular challenge. Eddy-current separation can be used to extract these metals from the remaining waste. In automotive waste, this fraction typically contains valuable metals such as high concentrations of aluminium, and other metals such as copper, and brass. Given the value of these metals, there is significant economic value in being able to further separate this fraction into its individual metal constituents.

We investigate the feasibility of classifying and sorting scrap non-magnetic metal targets by analysing the spectral response of the scattered magnetic field from an object when subjected to some oscillating excitation magnetic field. Classification based on spectral response has been investigated for identifying clutter in landmine detection [2], [3]. Further, we have previously used single-frequency magnetic polarisability tensor measurements [4] and fast boundary element solver for this application [5]. Our aim is to produce a fast and robust algorithm capable of the high-throughput processing typical and necessary in the waste recycling industry.

II. Theory

The classification algorithm is based on the scattered magnetic field induced in a non-magnetic conductive object subjected to an excitation magnetic field over a range of different frequencies. We term the response the impedance spectra as the scattered field relates to the impedance of the object with respect to the eddy-currents induced within by the excitation field.

Consider a non-magnetic conductive sphere placed at the origin, exposed to a uniform oscillating magnetic field $\mathbf{H}_{tx}e^{-j\omega t}$ acting along an axis Z. This *excitation field* induces eddy-currents in the sphere, which in turn, induce a secondary magnetic field $\mathbf{H}_S e^{-j\omega t}$ in a direction opposing the original excitation field. The net result is a magnetic field which appears to be forced or *scattered* around the object. We can show from Maxwell's equations that the secondary field is comparably weak when the excitation is low-frequency. The consequent net magnetic field can pass through or penetrate the object. However as the frequency increases, the net magnetic field is pushed increasingly out of the object until reaching an asymptotic case where no penetration occurs [5]. At this point, the object is equivalent to being a perfect electrical conductor.

Now consider a point some small distance from the surface of the sphere along the axis Z. By plotting the complex components of the secondary field with respect to the excitation ($\mathbf{H}_S/\mathbf{H}_{tx}$) at different frequencies, we can generate the impedance spectra shown in figure 1. The shape of the real and imaginary curves in this figure are characteristic for non-magnetic conductive objects [3], [6] .

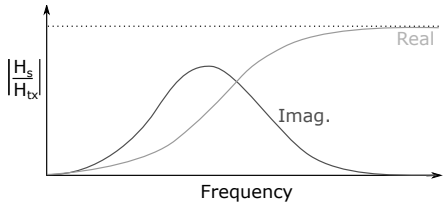

Fig. 1. Typical impedance spectra of a non-magnetic conductive object

We make two observations: (1) The imaginary component at frequencies along the loss-curve is a function of the conductivity and geometry of the object, and (2) the real component at high frequencies - close to the asymptote - is insensitive to conductivity and is mostly a function of the object geometry. This is because at high frequencies, the skin-depth is negligible and eddy-currents will only circulate along

the surface boundary. We propose that by comparing these two features, a simple classifier can by produced capable of classifying different non-magnetic conductive metals. In the present work, we specifically aim to classify aluminium, copper and brass targets.

III. Method

The impedance spectra is investigated using the quarter-length electromagnetic tensor spectroscopy (EMTS) experimental system shown in figure 3. Note that a large *industrial-scale* version of this system is described in a companion paper in the same proceedings.

A set of 36 test pieces (17 aluminium, 13 brass and 6 copper) are scanned using the system. The pieces are shown in figure 2. They are of varied sizes and shapes but are all between 10-30 mm in width or length and >2mm height. The size specification of the pieces is a realistic representation of a fraction-size in the scrap metal sorting industry. Some of the test pieces are also painted black as shown in figure 2 to ensure they are detected by the camera.

Fig. 2. Test samples. Sixteen Aluminium (left), fourteen brass (right), and six copper pieces (top).

The system is shown in figure 3. A test piece is dropped on to the right-hand-side (according to the image) of a conveyor running at approximately 1 m/s. The piece is conveyed first towards a camera system which logs the position of the object across the 100 mm width of the belt and alerts the system to start recording measurements. The piece is then conveyed across the sensor array sited underneath the belt. The sensor array emits a multi-frequency excitation magnetic field which in turn induces eddy-currents and a secondary magnetic field in the test piece. The array then detects the secondary magnetic field which is used to obtain a six-point impedance spectra of the object at 2 kHz, 4 kHz, 8 kHz, 16 kHz, 32 kHz and 64 kHz. Once the object has passed the sensor array, the system ceases recording and returns the six-point spectra to the control computer.

The inside of the sensor array is shown in figure 4. The main components are four solenoids situated vertically and evenly spaced underneath and across the 100 mm width of the belt. Each solenoid is constructed of an internal 8 mm diameter ferrite core with an 84 turn coil wrapped across approximately 80 mm length. This is the excitation coil and its purpose is to generate a multi-frequency excitation magnetic field. It is driven with a six frequency multi-sine waveform using a power amplifier (Linear Technologies LT1210) situated in the electronics enclosure (figure 3).

The internal core is inserted into a 16mm diameter outer core with two 600-turn coils wrapped on either end. These are the receive coils which detect the secondary magnetic field emitted by the object. They are wound in opposing directions to one another and connected together in the manner of a gradiometer to reduce or remove the effect of the primary excitation magnetic field. They are then connected to a low-noise differential amplifier (Analog device AD8049) housed on the rear side (not pictured) of the sensor array.

Control of the system and signal processing are performed by a ADC/DAC + FPGA system (NI PXI 1033 with NI PXI 7853R module, National Instruments) and desktop computer. The system is calibrated by passing a small ferrite bead (Ferroxcube 4B1) across the top of the coils to compensate for magnitude and phase-shifts present in the system (e.g. see [7]).

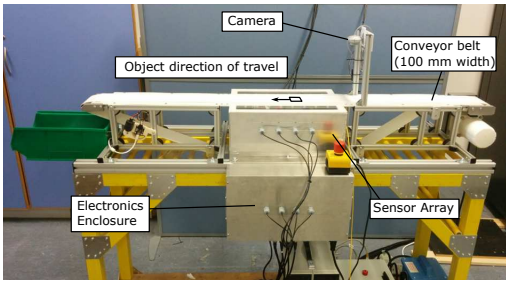

Fig. 3. The quarter-length electromagnetic tensor spectroscopy (EMTS) experimental system created as part of the project SHREDDERSORT

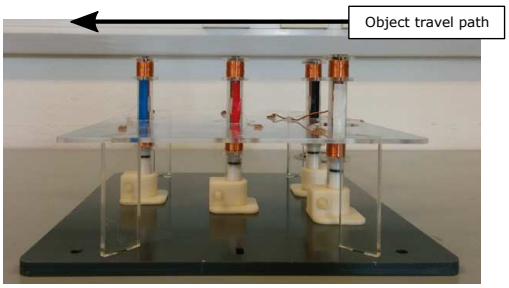

Fig. 4. The quarter-length electromagnetic tensor spectroscopy (EMTS) experimental system created as part of the project SHREDDERSORT

IV. Results and Discussion

We compare the real component of the spectra at 64 kHz ($Z'(64kHz)$) to the imaginary component at 16 kHz ($Z''(16kHz)$) following our observations in section 2. The real component at this frequency is close to the asymptote of the frequency response - as shown in figure 5 - and is insensitive to the conductivity of the test piece due to the negligible skin-depth of the circulating eddy-currents. The imaginary component at 16 kHz on the other-hand is sensitive to both the conductivity of the test piece and its shape.

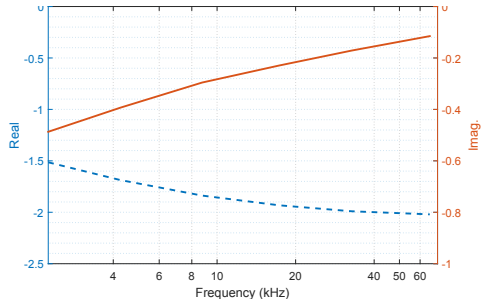

Fig. 5. Real and Imaginary Spectra of a 25 mm x 25 mm Aluminium cylinder.

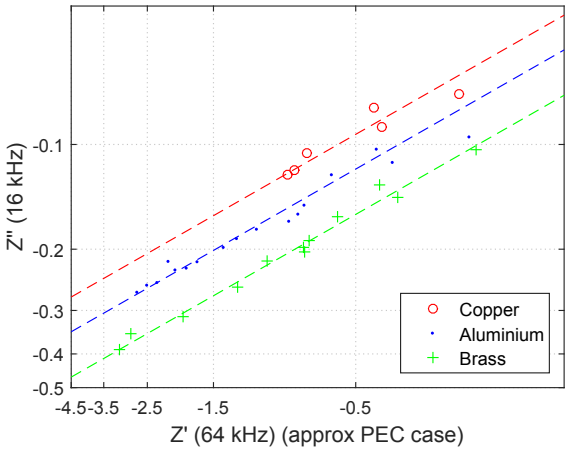

Fig. 6. Real component ($Z'(64kHz)$) vs Imaginary component $Z''(16kHz)$ for Cu, Al and Br. Dashed lines show the best fit for each metal.

The two frequency components are compared in figure 6. The figure shows clear evidence of each of the three metal groups converging along a band in order of conductivity from the highest (copper) to the lowest (brass). Figure 6 also shows lines-of-best-fit for each of the three metal types. Using the these lines we can approximate three functions for classification as follows,

$$C_{Cu} = 0.49\ln(|Z'_{64kHz}|) - \ln(|Z''_{16kHz}|) - 2.03$$
$$C_{Al} = 0.49\ln(|Z'_{64kHz}|) - \ln(|Z''_{16kHz}|) - 1.8$$
$$C_{Br} = 0.49\ln(|Z'_{64kHz}|) - \ln(|Z''_{16kHz}|) - 1.5$$

These functions are effectively distance measures from each line-of-best fit. The class of a test piece can be determined by which line it falls closest to. Thus we derive the following simple classifier,

$$\textbf{Class} := \arg\min\{C_{Cu}, C_{Al}, C_{Br}\}$$

Classifying the test pieces using this method results in the confusion matrix shown in table I. A total of 94.4% of pieces were correctly classified overall with 83.3% of copper correctly classified, 94.1% aluminium and 100% brass. In this case, we have not separated the test pieces into training and test sets due to the limited number of test pieces available in this preliminary study. We note however, that the lines of best fit presented in figure 6 have small residuals and no significant outliers. The results therefore would be unlikely to change by using a leave-one-out or other similar methods typically used with small data sets.

Pred. Class \ Target Class	Cu	Al	Br	
Cu	5	0	0	100%
Al	1	16	0	94.1%
Br	0	1	13	92.9%
	83.3%	94.1%	100%	94.4%

TABLE I
CONFUSION MATRIX

V. CONCLUSION

We demonstrate the feasibility of a fast and simple algorithm for classifying small non-magnetic conductive metal test pieces equivalent to a 10-30 mm scrap fraction size. Using an experimental test system, we are able to extract robust impedance spectrum of metal test objects as they pass over a sensor array at high speed (1 m/s).

The algorithm uses the real component of the spectra at a high-frequency (64 kHz) and the imaginary component at lower frequency (16 kHz) to create a set of conductivity bands which can be exploited to classify the test pieces as either copper, brass or aluminium. We find an overall 94.4% of pieces correctly classified in this study. The relatively high accuracy shown in the confusion matrix is a strong indicator that the proposed algorithm is both feasible and practical. However, the success rates must be judged with some caution given the small sample set available in this study.

ACKNOWLEDGMENTS

This research was funded by the project 'SHREDDER-SORT' under the EU seventh Framework Programme grant no. 603676.

REFERENCES

[1] E. Commission, *Report from the Commission to the Council and the European Parliament on sustainability requirements for the use of solid and gaseous biomass sources in electricity, heating and cooling*. Publications Office of the European Union, 2010.

[2] L. A. Marsh, J. L. Davidson, M. D. O'Toole, A. J. Peyton, D. Ambras, D. Vasic, and V. Bilas, "Spectroscopic identification of anti-personnel mine surrogates from planar sensor measurements," in *2016 IEEE SENSORS*, Oct 2016, pp. 1–3.

[3] O. A. Abdel-Rehim, J. L. Davidson, L. A. Marsh, M. D. OToole, and A. J. Peyton, "Magnetic polarizability tensor spectroscopy for low metal anti-personnel mine surrogates," *IEEE Sensors Journal*, vol. 16, no. 10, pp. 3775–3783, May 2016.

[4] J. Makkonen, L. A. Marsh, J. Vihonen, M. D. O'Toole, D. W. Armitage, A. Jrvi, A. J. Peyton, and A. Visa, "Determination of material and geometric properties of metallic objects using the magnetic polarisability tensor," in *2015 IEEE Sensors Applications Symposium (SAS)*, April 2015, pp. 1–5.

[5] M. D. O'Toole, J. L. Davidson, L. A. Marsh, W. Yin, and A. J. Peyton, "Evaluation of the thin-skin approximation boundary element method for electromagnetic induction scattering problems," in *2016 IEEE Sensors Applications Symposium (SAS)*, April 2016, pp. 1–6.

[6] J. R. Wait, "A conducting permeable sphere in the presence of a coil carrying an oscillating current," *Canadian Journal of Physics*, vol. 31, no. 4, pp. 670–678, 1953.

[7] M. D. O'Toole, L. A. Marsh, J. L. Davidson, Y. M. Tan, D. W. Armitage, and A. J. Peyton, "Non-contact multi-frequency magnetic induction spectroscopy system for industrial-scale bio-impedance measurement," *Measurement Science and Technology*, vol. 26, no. 3, p. 035102, 2015.